 CMC, vol.40, no.2, pp.131-143, 2014

Graded Dielectric Inhomogeneous Planar Layer Radome for Aerospace Applications

Raveendranath U. Nair, Preethi D.S, and R. M. Jha

Abstract: Controllable artificial dielectrics are used in the design of radomes to enhance their electromagnetic (EM) performance. The fabrication of such radome wall structures with controllable dielectric parameters seems to be an arduous task. Further even minor fluctuations of dielectric properties of radome wall due to fabrication uncertainties tend to result in drastic degradation of radome performance parameters. In the present work, a novel inhomogeneous radome with graded variation of dielectric parameters is proposed which limits the constraints on fabrication and facilitates excellent EM performance characteristics. This radome wall consists of five dielectric layers cascaded such that the middle layer has maximum dielectric constant and electric loss tangent. The dielectric parameters of the layers on both sides of the middle layer decrease in a graded (or step-wise) manner. The EM performance characteristics of the IPL radome with graded dielectric parameters are superior to that of conventional monolithic half-wave radome.

Keywords: Inhomogeneous planar dielectric radome, Equivalent transmission line model, EM performance parameters.

1 Introduction

Several techniques for broadbanding of radomes based on metallic wire grids/ meshes, resonant/ semi-resonant inclusions, anisotropic materials are reported in the open literature [Walton (1966); Bodnar and Basset (1975); Cary (1983); Kozakoff (2010)]. Due to superior filter (band-pass/ band-stop) characteristics, both conventional and metamaterial based frequency selective surfaces are widely used in the design of radomes [Cory *et al*. (2007); Basiry *et al*. (2011); Costa and Monorchio (2012), Narayan *et al*. (2012); Nair *et al*. (2013)]. Further, materials/ structures with controllable dielectric properties have been used in the design of radome wall configurations to meet the high-end electromagnetic (EM) performance requirements of modern radar antenna systems [Chen *et al*. (2010); Pei *et al*. (2012)]. The practical realization of radome wall configurations with control-

lable dielectric characteristics is often a challenging problem [Nair *et al.* (2012)]. In the present work, inhomogeneous planar layer (IPL) radome wall configuration with graded dielectric parameters is proposed, which can be easily fabricated by cascading different dielectric layers (Fig.1). Here the dielectric parameters are increased from the outer wall to the middle layer in a graded manner (or step-wise variation). The EM performance analysis indicates that the graded dielectric IPL radome wall configuration has superior EM performance parameters as compared to that of conventional monolithic half-wave radome of identical thickness.

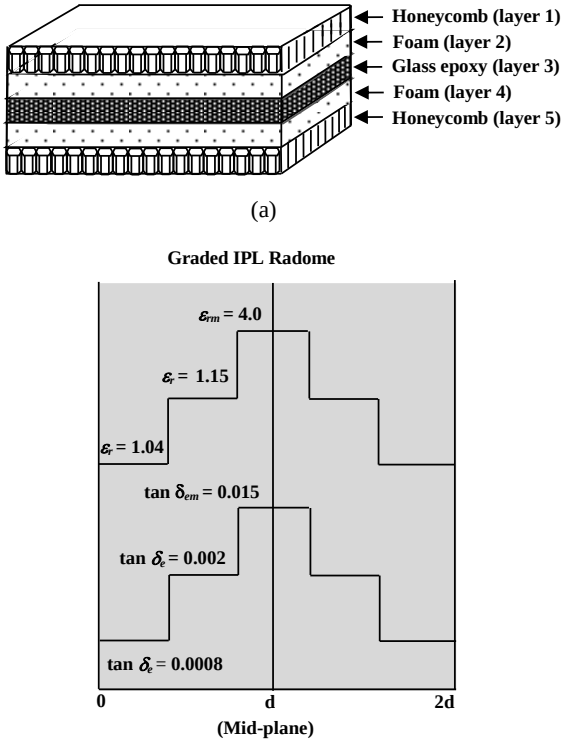

Figure 1: (a) Schematic of graded dielectric IPL radome and (b) Graded variation of dielectric parameters across the radome wall.

2 Graded Dielectric IPL Radome: EM Design Aspects

The radome wall consists of five cascaded dielectric layers with different dielectric properties (Fig. 1a). The total thickness of the entire radome wall is 7.44 m-

m, which is the optimized thickness of conventional monolithic half-wave radome (design frequency of 10 GHz). Both Layer 1 and Layer 5 are made of quartz honeycomb (dielectric constant, ε_r = 1.04; and loss tangent, tan δ_e = 0.0008). Layer 2 and Layer 4 are made of polyurethane foam (ε_r = 1.15 and tan δ_e = 0.002). Layer 3 (central layer) is made of glass epoxy having the highest dielectric parameters (ε_{rm} = 4.0 and tan δ_{em} = 0.015). Thus graded (or step-like) variation of dielectric parameters is incorporated in the radome wall (Fig. 1b).

Table 1: Optimized design parameters of graded IPL radome (Polarization: perpendicular).

Layer	Material	Thickness (mm)	Dielectric Constant	Loss tangent
Layer 1	Quartz Honeycomb	2	1.04	0.0008
Layer 2	PU Foam	1.57	1.15	0.002
Layer 3	Glass Epoxy	0.3	4.0	0.015
Layer 4	PU Faom	1.57	1.15	0.002
Layer 5	Quartz Honeycomb	2	1.04	0.0008

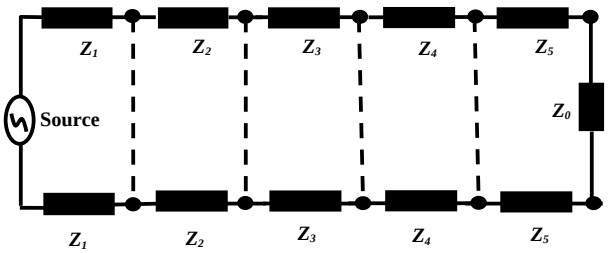

Figure 2: Equivalent transmission line model of graded dielectric IPL radome.

The graded dielectric IPL radome is modeled as an equivalent transmission line with different sections corresponding to respective dielectric layers (Fig. 2). The radome performance parameters are computed using equivalent transmission line model [Nair *et al*. (2012)]. The voltage-current transmission matrix of the entire graded dielectric IPL radome wall is obtained as,

$$\begin{bmatrix} A & B \\ C & D \end{bmatrix} = \begin{bmatrix} \cos\varphi_1 & j\frac{Z_1}{Z_0}\sin\varphi_1 \\ j\frac{Z_1}{Z_0}\sin\varphi_1 & \cos\varphi_1 \end{bmatrix} \begin{bmatrix} \cos\varphi_2 & j\frac{Z_2}{Z_0}\sin\varphi_2 \\ j\frac{Z_2}{Z_0}\sin\varphi_2 & \cos\varphi_2 \end{bmatrix} \begin{bmatrix} \cos\varphi_3 & j\frac{Z_3}{Z_0}\sin\varphi_3 \\ j\frac{Z_3}{Z_0}\sin\varphi_3 & \cos\varphi_3 \end{bmatrix} \begin{bmatrix} \cos\varphi_4 & j\frac{Z_4}{Z_0}\sin\varphi_4 \\ j\frac{Z_4}{Z_0}\sin\varphi_4 & \cos\varphi_4 \end{bmatrix} \begin{bmatrix} \cos\varphi_5 & j\frac{Z_5}{Z_0}\sin\varphi_5 \\ j\frac{Z_5}{Z_0}\sin\varphi_5 & \cos\varphi_5 \end{bmatrix} \tag{1}$$

Here Z_1, Z_2, Z_3, Z_4, and Z_5 are the intrinsic impedances of the layers. Z_0 is the freespace impedance. The electrical length ϕ of each layer is a function of the thickness, complex permittivity, angle of incidence, and wavelength of incident wave.

The power transmission is expressed as

$$P_{tr} = \left| \left(\frac{2}{A+B+C+D} \right) \right|^2 \tag{2}$$

Similarly, the power reflection is given by

$$P_{rf} = \left| \left(\frac{A+B-C-D}{A+B+C+D} \right) \right|^2 \tag{3}$$

The insertion phase delay (IPD) of the graded dielectric IPL radome is given by

$$\begin{aligned} IPD = &- (\angle T_1 + \angle T_2 + \angle T_3 + \angle T_4 + \angle T_5) \\ &- \frac{2\pi}{\lambda} (d_1 \cos\theta_1 + d_2 \cos\theta_2 + d_3 \cos\theta_3 + d_4 \cos\theta_4 + d_5 \cos\theta_5) \end{aligned} \tag{4}$$

Here $\angle T_1$, ..., $\angle T_5$ are the phase angles associated with the voltage transmission coefficients of the dielectric layers with thicknesses d_1, ...,d_5 respectively. θ_1,...,θ_5 are the corresponding incidence angles at the interfaces of the dielectric layers.

3 EM Performance Analysis

The EM performance envelopes corresponding to power transmission, power reflection, and IPD characteristics of graded dielectric IPL radome, and monolithic half-wave radome of identical thickness over the entire range of incidence angles from 0° to 80° and X-band are shown in Figures 3 through 5. Since the EM performance degradation for perpendicular polarization represents the worst-case scenario, the EM performance parameters are analyzed only for perpendicular polarization in the present work.

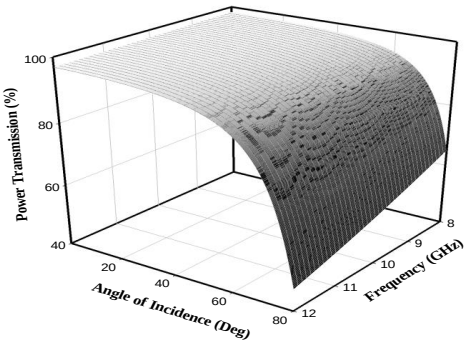

Figure 3: Power Transmission characteristics of graded IPL radome over a wide range of incidence angles and X-band (Polarization: perpendicular).

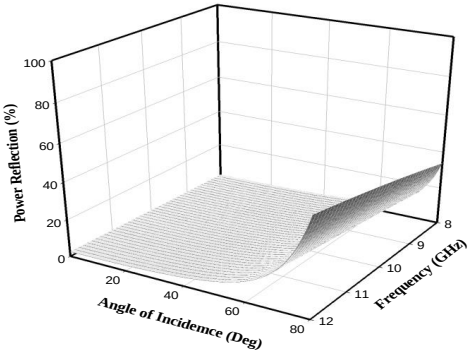

Figure 4: Power reflection characteristics of graded IPL radome over a wide range of incidence angles and X-band (Polarization: perpendicular).

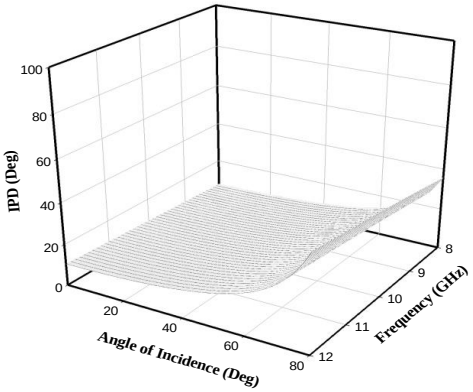

Figure 5: Insertion phase delay characteristics of graded IPL radome over a wide range of incidence angles and X-band (Polarization: perpendicular).

It is observed that the graded IPL radome shows excellent EM performance characteristics upto 60° incidence angle. However, there is a drastic degradation of performance parameters beyond 60°. A comparative study of EM performance parameters (power transmission, power reflection, and IPD) of graded dielectric IPL radome, and monolithic half-wave radome has been carried out at normal incidence, 30°, 45°, and at high incidence angle 60° in the figures below.

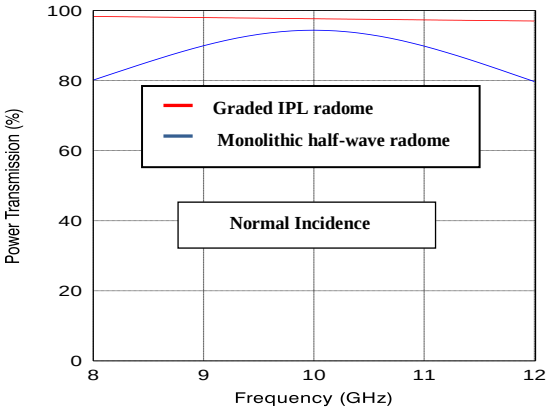

Figure 6: Power transmission characteristics of graded IPL radome and monolithic half-wave radome at normal incidence.

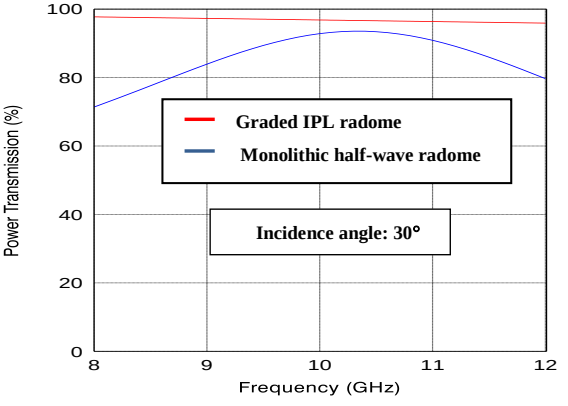

Figure 7: Power transmission characteristics of graded IPL radome and monolithic half-wave radome at incidence angle 30° (Polarization: perpendicular).

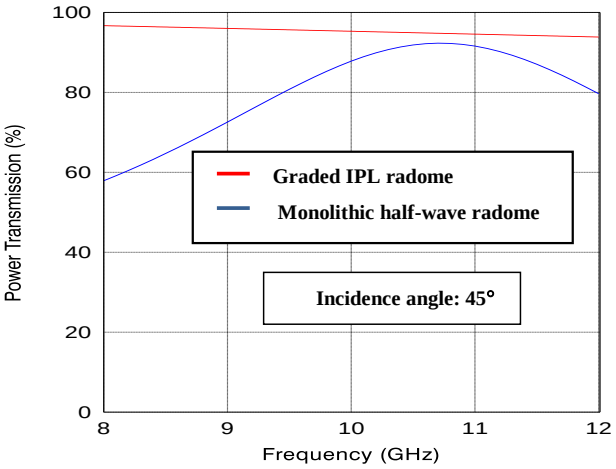

Figure 8: Power transmission characteristics of graded IPL radome and monolithic half-wave radome at incidence angle 45˚ (Polarization: perpendicular).

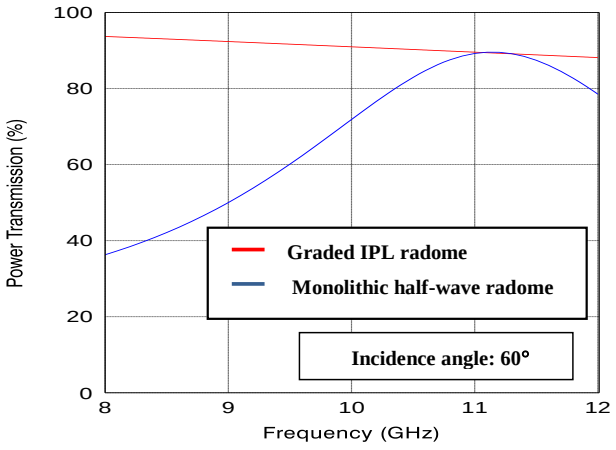

Figure 9: Power transmission characteristics of graded IPL radome and monolithic half-wave radome at incidence angle 60˚ (Polarization: perpendicular).

The power transmission efficiency of graded dielectric IPL radome is superior to that of conventional monolithic radome at both the normal incidence and high incidence angles representing different classes of radome applications (Figures 6-9). It is pointed out that the transmission efficiency of graded dielectric IPL radome is above 90% in the entire X-band. Such high transmission efficiency, over wideband and a range of incidence angles, is required for modern radome applications.

Low power reflection characteristic is achieved for the graded IPL radome design at both normal incidence, and high incidence angles over the entire X-band frequency regime (Figures 10-13).

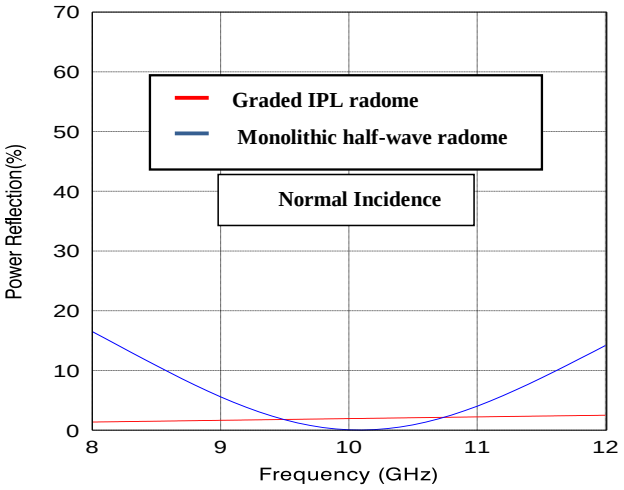

Figure 10: Power reflection characteristics of graded IPL radome and monolithic half-wave radome at normal incidence.

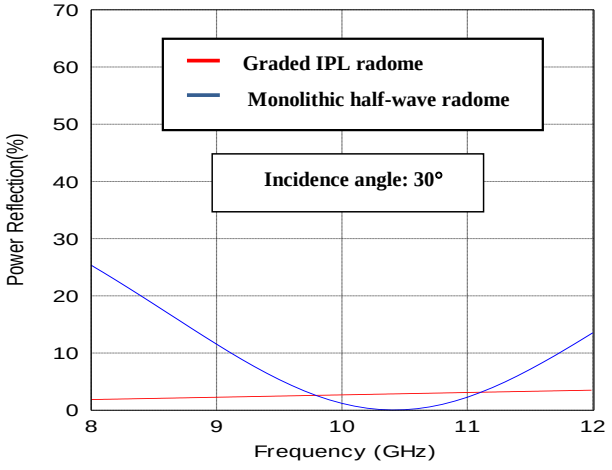

Figure 11: Power reflection characteristics of graded IPL radome and monolithic half-wave radome at incidence angle 30° (Polarization: perpendicular).

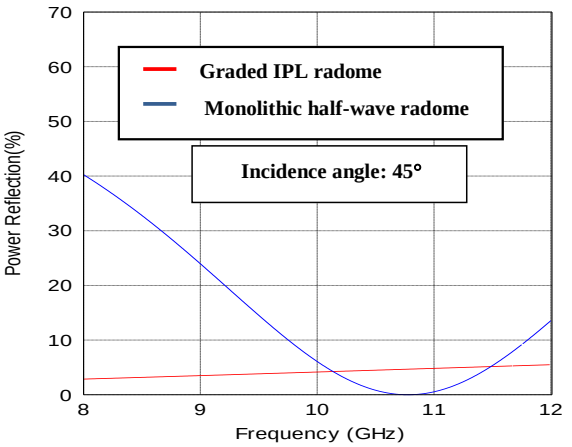

Figure 12: Power reflection characteristics of graded IPL radome and monolithic half-wave radome at incidence angle 45˚ (Polarization: perpendicular).

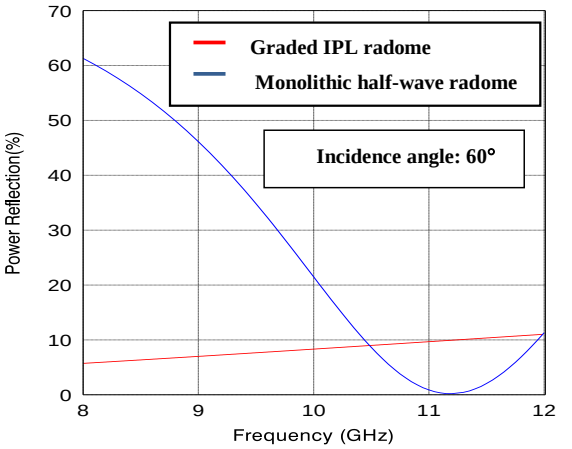

Figure 13: Power reflection characteristics of graded IPL radome and monolithic half-wave radome at incidence angle 60˚ (Polarization: perpendicular).

Such low power reflection characteristics are desirable for radome applications as it facilitates the reduction of sidelobe level (SLL) degradations of antenna radiation pattern, minimization of pattern ripples, and elimination of flash lobes in the scan volume. The variation of IPD for graded dielectric IPL radome over the X-band frequency range is less than that of monolithic radome (Figures 14-17). Such IPD characteristics (low magnitude and small variation across the entire X-band)

indicate low phase distortions, which in turn reduces the boresight error (BSE) for streamlined nosecone radomes for airborne applications.

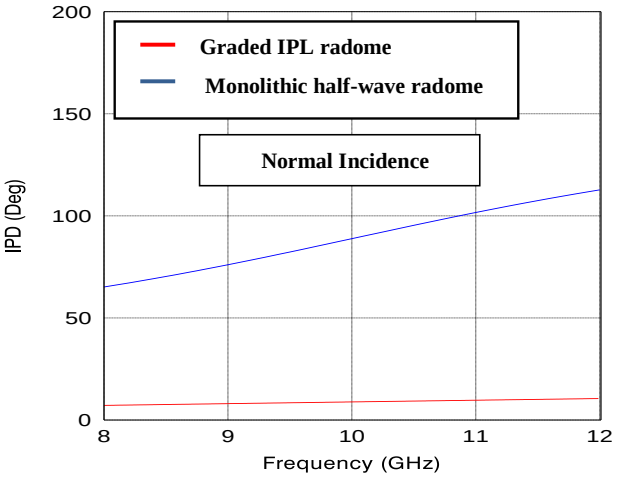

Figure 14: Insertion phase delay characteristics of graded IPL radome and monolithic half-wave radome at normal incidence.

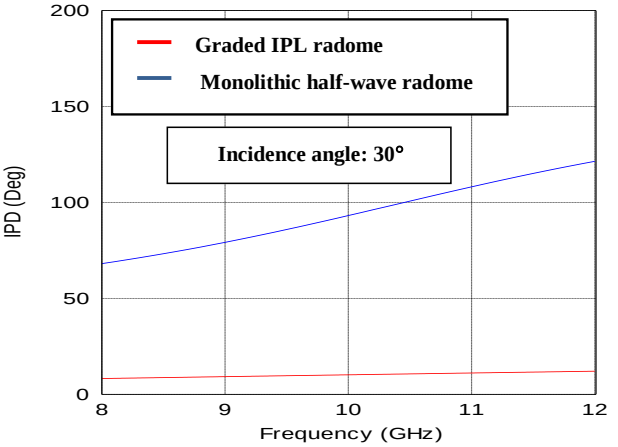

Figure 15: Insertion phase delay characteristics of graded IPL radome and monolithic half-wave radome at incidence angle 30° (Polarization: perpendicular).

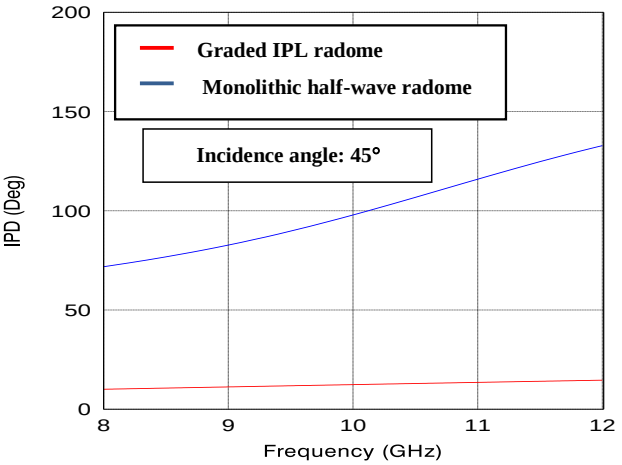

Figure 16: Insertion phase delay characteristics of graded IPL radome and monolithic half-wave radome at incidence angle 45˚ (Polarization: perpendicular).

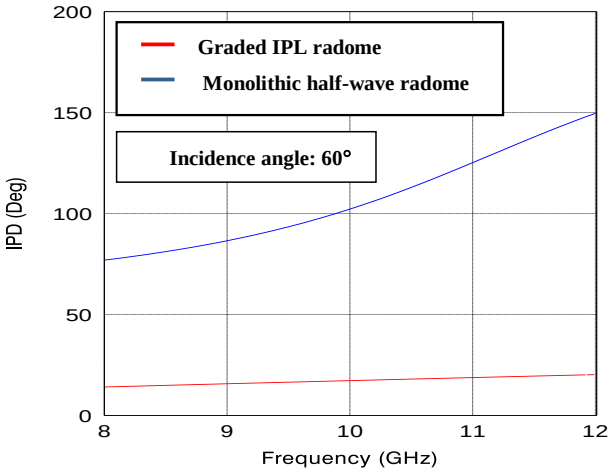

Figure 17: Insertion phase delay characteristics of graded IPL radome and monolithic half-wave radome at 60˚ (Polarization: perpendicular).

4 Conclusion

The present work shows that the graded IPL radome has superior EM performance characteristics at both the normal and high incidence angles, as compared to the conventional monolithic radome. This establishes that the graded IPL radome wall

configuration has promising application in the design of hemispherical, cylindrical radomes and streamlined nosecone radomes. Since this structure offers superior power transmission and low IPD characteristics, it has also potential application in the design of walls for structurally integrated radiating systems for aircraft and coverings for embedded antennas in aircraft wing and fuselage.

References

Basiry, R.; Abiri, H.; Yahaghi, A. (2011): Electromagnetic performance analysis of omega type metamaterial radome. *International Journal of RF and Microwave Computer-Aided Engineering,* vol. 21, no. 6, pp. 665-673.

Bodnar, D. G.; Basset, H. L. (1975): Analysis of an anisotropic dielectric radome. *IEEE Transactions on Antennas and Propagation,* vol. 23, pp. 841-846.

Cary, R. H. J. (1983): Radomes, *The Handbook of Antenna Design.* Peter Peregrinus, London, ISBN 0-906048-87-7, p. 930.

Chen, F.; Shen, Q.; Zhang, L. (2010): Electromagnetic optimal design and preparation of broadband ceramic radome material with graded porous structure. *Progress in Electromagnetics Research*, vol. 105, pp. 445-461.

Cory, S.; Lee, Y. J.; Hao, Y.; Parini, C. G. (2007): Use of conjugate dielectric and metamaterial slabs as radomes. *IET Microwaves, Antennas, and Propagation,* vol. 1, no. 1, pp. 137-143.

Costa, F.; Monorchio, A. (2012): A frequency selective radome with wideband absorbing properties. *IEEE Transactions on Antennas and Propagation*, vol. 60, no. 6, pp. 2740-2747.

Kozakoff, D. J. (2010): *Analysis of radome enclosed antennas* , Artech House, Norwood, USA, ISBN 13: 978-1-59693-441-2, p. 318.

Nair, R. U.; Sandhya, S.; Jha, R. M. (2012): Novel inhomogenous planar layer radome design for airborne applications. *IEEE Antennas and Wireless Propagation Letters,* vol. 11, no. 1, pp. 854-856.

Nair, R. U.; Jha, R. M. (2013): Broadbanding of A-sandwich radome using Jerusalem cross frequency selective surface. *Computers, Materials & Continua,* vol. 37, no. 2, pp. 109-121.

Narayan, S.; Shamala, J. B.; Nair, R. U.; Jha, R. M. (2012): Electromagnetic performance analysis of novel multiband metamaterial FSS for millimeter wave radome applications. *Computers, Materials & Continua,* vol. 31, no. 1, pp. 1-16.

Pei, Y.; Zeng, A.; Zhou, L.; Zhang, R.; Xu, K. (2012): Electromagnetic optimal design for dual-band radome wall with alternating layers of staggered composite and Kagome lattice structure. *Progress in Electromagnetics Research*, vol. 122,

pp. 437-452.

Walton J. D. (1966): Techniques for airborne radome design. *AFAL Report,* no. 45433.